The Astrophysical Journal, 965:91 (6pp), 2024 April 10 https://doi.org/10.3847/1538-4357/ad344e

Supernova Burst and Diffuse Supernova Neutrino Background Simulator for Water Cherenkov Detectors

Fumi Nakanishi[1], Shota Izumiyama[2], Masayuki Harada[1], and Yusuke Koshio[1,3]
[1] Department of Physics, Okayama University, 3-1-1 Tsushima-naka, Kita-ku, Okayama, Okayama 700-8530, Japan; nakanishi-suv@s.okayama-u.ac.jp
[2] Department of Physics, Tokyo Institute of Technology, 2-12-1 H-26, Ookayama, Meguro-ku, Tokyo, 152-8551, Japan
[3] Kavli Institute for the Physics and Mathematics of the Universe (WPI), The University of Tokyo Institutes for Advanced Study, University of Tokyo, Kashiwa, Chiba 277-8583, Japan
Received 2024 January 31; revised 2024 March 8; accepted 2024 March 11; published 2024 April 10

Abstract

If a Galactic core-collapse supernova explosion occurs in the future, it will be critical to rapidly alert the community to the direction of the supernova by utilizing neutrino signals in order to enable the initiation of follow-up optical observations. In addition, there is anticipation that observation of the diffuse supernova neutrino background will yield discoveries in the near future, given that experimental upper limits are approaching theoretical predictions. We have developed a new supernova event simulator for water Cherenkov neutrino detectors, such as the highly sensitive Super-Kamiokande. This simulator calculates the neutrino interaction in water for two simulation purposes, individual core-collapse supernova bursts and diffuse supernova neutrino background. Based on this simulator, we can evaluate the precision in determining the location of supernovae and estimate the expected number of events related to the diffuse supernova neutrino background in Super-Kamiokande. In this paper, we describe the basic structure of the simulator and its demonstration.

Unified Astronomy Thesaurus concepts: Supernova neutrinos (1666); Neutrino telescopes (1105); Astronomy software (1855)

1. Introduction

A core-collapse supernova (CCSN) is an explosion at the end of the evolution of a massive star and one of the most energetic astrophysical phenomena. It releases energy of $\sim 10^{53}$ erg in total, 99% of which is released as neutrinos. A supernova (SN), SN1987A, is the latest event that has been seen by eyes on the Earth. At that time, neutrino detectors, the Kamiokande-II (Hirata et al. 1987), the Irvine–Michigan–Brookhaven (Bionta et al. 1987), and the Baksan experiments (Alexeyev et al. 1988) observed neutrinos. Since these are the first and last observations so far of neutrinos from an SN, the mechanism of the explosion is not yet well understood. Due to the limitation of neutrino observations, studies that reveal the mechanism are based on state-of-the-art numerical simulations. Early studies assumed the spherical symmetry of stars, for example, in the Wilson model (Totani et al. 1998). Thanks to the recent development in computers, multidimensional simulations have been developed and are available (Takiwaki et al. 2012; Hanke et al. 2013; Tamborra et al. 2014; Burrows et al. 2020; Burrows & Vartanyan 2021). While simulation studies have made great progress, preparations for the next observations of CCSN neutrinos are ongoing. On the detector side, there are several large-volume neutrino telescopes in the world, such as Super-Kamiokande (SK; Fukuda et al. 2003), IceCube (Aartsen et al. 2017), KM3NeT (Adrián-Martínez et al. 2016), and KamLAND (Suzuki 2014). There are also alert systems for follow-up observatories using these telescopes. For example, SK has a real-time burst monitor and an alert system (Kashiwagi et al. 2024) via the Global Coordinates Network.[4] In addition, those large-volume neutrino detectors are coordinated in the SuperNova Early Warning System (Al Kharusi et al. 2021).

Furthermore, it is thought that neutrinos generated by past SNe have occurred in large numbers throughout the history of the Universe. The flux from these is called diffuse SN neutrino background (DSNB) or SN relic neutrino flux (Hartmann & Woosley 1997; Malaney 1997). To further improve the sensitivity to the DSNB observation, SK was upgraded by adding gadolinium (Gd), which has the largest thermal neutron capture cross section among all elements, to the water in the detector. This upgrade is called SK-Gd (Abe et al. 2022).

With the growth of detectors and SN models, simulators of open software that connect SN simulation and detector response have also been developed, such as sntools (Migenda et al. 2021), SNEWPY (Baxter et al. 2022), and SNOWGLOBES (Scholberg et al. 2021), for individual SN explosions (SN bursts). The above tools are highly versatile software programs that enable SN neutrino simulations such as event generation by automatically matching the channels that can be observed by each SN neutrino detector, including water Cherenkov, liquid scintillator, and water-based liquid scintillator.

We have developed an SK SuperNova Simulator (SKSNSim)[5] which is an event generator for SN bursts and DSNBs. SKSNSim, originally developed for SK, is a simulator of neutrino interactions in water Cherenkov neutrino detectors and applies to any water-medium detectors. The goal of SKSNSim is to make SN neutrino event generation in water Cherenkov detectors more realistic by introducing all possible interactions, including those with oxygen nuclei, and also to handle SN bursts and DSNBs in a unified manner. In this paper, we describe the details of this simulator. Section 2 presents the

[4] General Coordinates Network (GCN), https://gcn.nasa.gov/.
[5] Available on GitHub, https://github.com/SKSNSim/SKSNSim.

simulation strategy and flow. We show the demonstration of simulation and its usage in Section 3. Finally, we summarize in Section 4.

2. The Structure of the Simulation Suite

SKSNSim is a simulator that calculates the kinematics of particles generated by neutrino interactions from the input flux of an SN burst or DSNB and outputs them. In this section, we explain the structure and flow of the simulation, which incorporates neutrino fluxes, neutrino oscillation effects along the propagation from the center of the star to its surface, as well as the interaction cross section in water. Because the SN burst and DSNB pipelines share some parts, like cross sections and methods to generate particles, SKSNSim is set up to deal with both cases.

We have implemented the main parts of SKSNSim using C++ programming language. The cross-section model and output formats are modularized, making it easy to use them in external programs and update the models.

2.1. Flow of the Simulation Software

The software can be run in two modes: either for the simulation of individual SN bursts or for the simulation of the DSNB. While some parts are common for both modes, there is a major difference: the SN burst flux is a function of time with subsecond precision, whereas the DSNB flux is constant in time.

The SN burst simulation consists of the following steps: (1) the calculation of the average number of interacting neutrinos for each neutrino type in the defined time and energy bins from the neutrino flux, cross section, and neutrino oscillation effects, (2) the estimation of the number of interacting neutrinos by throwing in a random number according to a Poisson distribution, (3) the determination of the kinematics of particles, such as vertex and momentum, generated in each event using random numbers, randomly produced according to the cross section. The sequence of steps (1)–(3) is repeated over the burst duration.

The following steps are used for the DSNB simulation: (1) randomization of the neutrino energy according to the chosen energy spectrum and (2) the determination of the kinematics of the particle randomly produced according to the cross section. Steps (1)–(2) are repeated as specified by the user. In this case, the final number of events must be normalized by the observation time. In contrast to the SN burst steps, the DSNB steps do not include the neutrino oscillation effect in SKSNSim because most DSNB models include it already.

2.2. Choice of SN Model

There is a variety of models, both for the SN burst and the DSNB, based on different simulation approaches. In dealing with any model, SKSNSim requires the original neutrino flux information for each time and energy in the SN burst simulation. In the case of the DSNB simulation, the neutrino flux information for each energy is necessary. The details about the input models for the SN burst and the DSNB cases are discussed in the following subsections.

2.2.1. SN Burst Case

Many SN burst modelers publish their results with data tables containing time from core bounce and the mean energy for each neutrino species to express the simulation results. We decided to support only the text format distributed by Nakazato et al. (2013) in the SN burst simulation to handle all models in a unified manner. This format includes differential neutrino number flux and differential neutrino luminosity for every time and energy bin and types of neutrino ν_e, $\bar{\nu}_e$, ν_x, $\bar{\nu}_x$. Here, ν_x represents ν_μ (ν_τ) because the distributions of ν_μ and ν_τ are equal, and also ν_μ and ν_τ of $\mathcal{O}10$ MeV behave the same way in water Cherenkov detectors. The conversion to the input data format is detailed in Kashiwagi et al. (2024). At this time, SN burst models listed in Table 1 are implemented in SKSNSim, and models will be added in the future.

Table 1
List of Current Supported SN Burst Models

Model	Supported Configuration	References
Nakazato	All parameters in the reference	Nakazato et al. (2013)
Mori	9.6 $M_\odot$	Mori et al. (2021)
Wilson	20 $M_\odot$	Totani et al. (1998)
Tamborra	27 $M_\odot$ and "black" observer direction	Tamborra et al. (2014)
Fischer	8.8 $M_\odot$	Fischer et al. (2010)
Hüdepohl	Full neutrino interactions and 8.8 $M_\odot$	Nomoto (1987)

Note. Except for the Nakazato and Mori models, the flux variation is converted to the format defined by Nakazato et al. (2013).

2.2.2. DSNB Case

The time dependence of the DSNB flux is negligible for a typical observation period of ∼10 yr, such as for SK. Therefore, SKSNSim simulates DSNB events using tabulated energy spectra without any time dependence. In addition, the DSNB simulation processes only the $\bar{\nu}_e$ flux since the inverse beta decay (IBD) is the dominant interaction in the typical energy range of DSNB neutrinos of a few tens of MeV. Users can specify any binned $\bar{\nu}_e$ spectrum to simulate the IBD interaction via a text file. This feature allows one to simulate the flux of other $\bar{\nu}_e$ sources, such as nuclear reactors, with this tool. By default, it supports the $\bar{\nu}_e$ flux model provided by Horiuchi et al. (2009). Another characteristic of SKSNSim is that it is implemented to simulate events according to a flat energy spectrum in a positron energy space as well as a neutrino energy space. This implementation is useful in the "reweighting" method. We explain in detail the use of the reweighting method for the SK DSNB analysis in Section 3.2.

2.3. Implementation of Neutrino Oscillation

As for the neutrino oscillations, there are oscillations during propagation in matter and a vacuum and collective oscillations (Duan et al. 2010). In SKSNSim, we only take into account the Mikheyev–Smirnov–Wolfenstein (MSW) effect (Wolfenstein 1978; Mikheyev & Smirnov 1985) inside the star. As described above, the neutrino oscillation effect is not included in the DSNB simulation. This section describes the treatment and implementation of the MSW effect in the simulation of an SN burst.

The following equations represent the neutrino flux, including the MSW effect, on the surface of the star ($N_\bullet^{\rm sur}$; Dighe & Smirnov 2000). Here, $N_{\nu_e}^{\rm gen}$, $N_{\bar{\nu}_e}^{\rm gen}$, and $N_{\nu_x}^{\rm gen}$ represent the neutrino flux of ν_e, $\bar{\nu}_e$, and ν_x at generation, respectively. In this notation, $N_{\nu_x}^{\rm gen}$ expresses the flux of ν_μ or ν_τ. The neutrino flux on the surface of the star in the normal mass ordering case

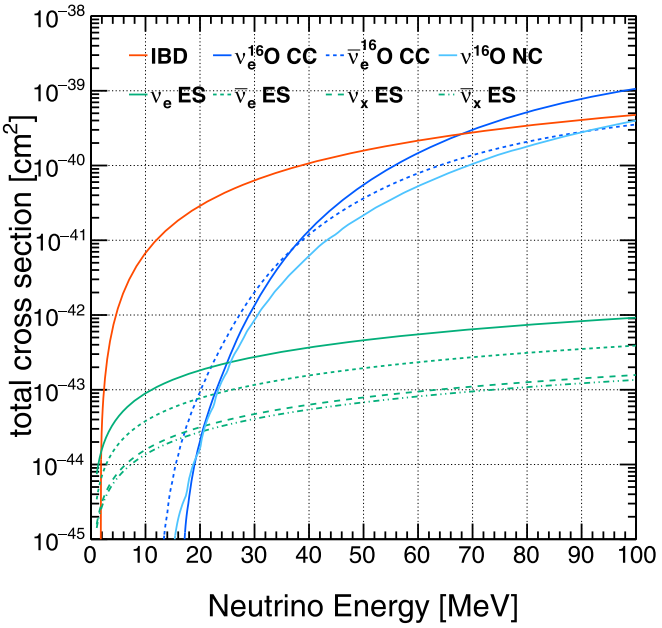

Figure 1. Total cross sections of neutrinos with water as a function of neutrino energy. The solid red line indicates IBD, and the green lines represent ES with a neutrino flavor: ν_e (solid), $\bar{\nu}_e$ (dotted), ν_x (dashed), and $\bar{\nu}_x$ (dotted–dashed). The solid blue and dashed blue lines represent ^{16}O CC ν_e and $\bar{\nu}_e$, respectively. The dotted–dashed light blue line indicates ^{16}O NC interaction. The cross sections are calculated according to Strumia & Vissani (2003) for IBD, Bahcall et al. (1995) for ES, Nakazato et al. (2018) for ^{16}O CC interaction, and Langanke et al. (1996) and Kolbe et al. (2002) for ^{16}O NC interaction.

is given by

$$\begin{aligned} N^{\rm sur}_{\nu_e} &= N^{\rm gen}_{\nu_x} \\ N^{\rm sur}_{\nu_\mu} + N^{\rm sur}_{\nu_\tau} &= N^{\rm gen}_{\nu_e} + N^{\rm gen}_{\nu_x} \\ N^{\rm sur}_{\bar{\nu}_e} &= N^{\rm gen}_{\bar{\nu}_e} \times \cos^2\theta_{12} + N^{\rm gen}_{\bar{\nu}_x} \times \sin^2\theta_{12} \\ N^{\rm sur}_{\bar{\nu}_\mu} + N^{\rm sur}_{\bar{\nu}_\tau} &= N^{\rm gen}_{\bar{\nu}_e} \times \sin^2\theta_{12} + N^{\rm gen}_{\bar{\nu}_x} \times (1 + \cos^2\theta_{12}). \end{aligned} \tag{1}$$

In contrast, in the inverted mass ordering case, the neutrino flux represents

$$\begin{aligned} N^{\rm sur}_{\nu_e} &= N^{\rm gen}_{\nu_e} \times \sin^2\theta_{12} + N^{\rm gen}_{\nu_x} \times \cos^2\theta_{12} \\ N^{\rm sur}_{\nu_\mu} + N^{\rm sur}_{\nu_\tau} &= N^{\rm gen}_{\nu_e} \times \cos^2\theta_{12} + N^{\rm gen}_{\nu_x} \times (1 + \sin^2\theta_{12}) \\ N^{\rm sur}_{\bar{\nu}_e} &= N^{\rm gen}_{\bar{\nu}_x} \\ N^{\rm sur}_{\bar{\nu}_\mu} + N^{\rm sur}_{\bar{\nu}_\tau} &= N^{\rm gen}_{\bar{\nu}_e} + N^{\rm gen}_{\bar{\nu}_x}. \end{aligned} \tag{2}$$

In SKSNSim, the oscillation effect is considered by multiplying by the coefficients specified in Equations (1) and (2). The oscillation effect (normal mass ordering, inverted mass ordering, and no oscillation) can be selected by the user.

2.4. Implementation of Neutrino Interactions

We consider the following four types of neutrino interactions in SKSNSim with a large cross section in the SN neutrino energy region observed in water. Figure 1 shows the cross section for each interaction.

Inverse Beta Decay

$$\bar{\nu}_e + p \rightarrow n + e^+, \tag{3a}$$

Electron scattering

$$\nu_e/\bar{\nu}_e/\nu_x/\bar{\nu}_x + e^- \rightarrow \nu_e/\bar{\nu}_e/\nu_x/\bar{\nu}_x + e^-, \tag{3b}$$

Charged−current reaction

$$\nu_e/\bar{\nu}_e + ^{16}\mathrm{O} \rightarrow e^-/e^+ + ^{16}\mathrm{F}/^{16}\mathrm{N}, \tag{3c}$$

Neutral−current reaction

$$\nu_e/\bar{\nu}_e/\nu_x/\bar{\nu}_x + ^{16}\mathrm{O} \rightarrow p/n + \gamma + ^{15}\mathrm{N}/^{15}\mathrm{O}. \tag{3d}$$

The IBD reaction has the largest cross section for the neutrinos with water. As a default, the cross section of IBD is calculated as below based on Strumia & Vissani (2003),

$$\frac{d\sigma}{dt} = \frac{G_{\rm F}^2 \cos^2\theta_{\rm C}}{2\pi(s - m_p^2)^2}|\mathcal{M}^2|, \tag{4}$$

where $G_{\rm F}$ is the Fermi coupling constant; $\theta_{\rm C}$ is the Cabibbo angle; s and t are the Mandelstam variables, which are functions of each particle's momentum; m_p is the proton mass; and $|\mathcal{M}|$ is the matrix element. The order of the IBD cross section is 10^{-41} cm^2 for the typical SN neutrino energies. SKSNSim includes the calculation by Vogel & Beacom (1999), Strumia & Vissani (2003; default in SKSNSim), and Ricciardi et al. (2022). Users can switch between these calculations.

Electron scattering (ES) is a reaction in which a neutrino scatters with an electron; all flavors of neutrino contribute to this interaction. The order of the cross section is 2 orders of magnitude lower than the IBD cross section. However, IBD has almost no directional sensitivity to the SN, whereas ES is characterized by a strong directional correlation between the neutrino and the scattered electron. The basic equation for the reaction cross section is derived from the weak interaction, and this generator uses the following equation that takes radiative corrections into account according to Bahcall et al. (1995),

$$\begin{aligned} \frac{d\sigma}{dT} = \frac{2G_{\rm F}^2 m_e}{\pi}\Bigg\{ & {g_L}^2(T)\left[1 + \frac{\alpha}{\pi}f_-(z)\right] \\ & + {g_R}^2(T)(1 - z)^2\left[1 + \frac{\alpha}{\pi}f_+(z)\right] \\ & - g_R(T)g_L(T)\frac{m_e}{q}z\left[1 + \frac{\alpha}{\pi}f_{+-}(z)\right]\Bigg\}, \end{aligned} \tag{5}$$

where m_e represents the electron mass, $T = E - m_e$ represents the kinetic energy of recoil electron, q represents incoming neutrino energy, and $z = T/q$. Also, g_L and g_R indicate the left-handed and right-handed electron weak couplings, respectively, and $f_{+,-,+-}$ are correction factors derived from QED. Equation (5) corresponds to neutrinos, while the cross section of antineutrinos corresponds to an interchange of g_L and g_R.

The charged-current reaction with oxygen (^{16}O CC) in the SN neutrino energy region is a process in which oxygen nuclei interact with neutrinos, leading to a giant resonance in which the entire assembly of nucleons resonates. In the case of charged-current reactions, an electron or positron is released from the oxygen nucleus for the charged-current reactions, and the nucleus changes to fluorine or nitrogen, respectively. Fluorine or nitrogen may be produced as excited states, of which there are many. When the fluorine or nitrogen exceeds the particle emission threshold, particles such as protons, neutrons, and alpha are emitted according to their respective thresholds. What is emitted from the nucleus is determined by

Table 2
List of Excited States Included in SKSNSim[a]

$^{16}O(\nu_e, e^- N'')N'$	0^- (MeV)	1^- (MeV)	2^- (MeV)	3^- (MeV)	1^+ (MeV)
	14.906	15.157	15.205	15.250	18.664
	27.580	20.567	19.413	...	19.431
	27.990	23.271	21.617	...	20.684
	...	25.514	22.473	...	21.937
	...	25.718	27.255	...	22.968
	...	26.728	27.823	...	24.431
	...	27.218	28.103	...	24.858
	...	28.141	28.922	...	25.772
	...	28.515	...	...	26.593
	...	29.200	...	...	27.412
	...	29.353	...	...	27.802
	...	29.975	...	...	28.082
	...	30.250	...	...	29.967
	...	30.803	...	...	31.084
	...	31.754	...	...	31.693
	...	...	...	...	32.981
$^{16}O(\bar{\nu}_e, e^+ N'')N'$	0^- (MeV)	1^- (MeV)	2^- (MeV)	3^- (MeV)	1^+ (MeV)
	10.932	11.183	11.231	11.276	14.285
	23.606	16.593	15.439	...	15.052
	24.016	19.297	17.643	...	16.305
	...	21.540	18.499	...	17.558
	...	21.744	23.281	...	18.589
	...	22.754	23.849	...	20.052
	...	23.244	24.129	...	20.479
	...	24.167	24.948	...	21.393
	...	24.541	...	...	22.214
	...	25.226	...	...	23.033
	...	25.379	...	...	23.423
	...	26.001	...	...	23.703
	...	26.276	...	...	25.588
	...	26.829	...	...	26.705
	...	27.780	...	...	27.314
	...	...	...	...	28.602

Note. This table shows excited states for $^{16}O(\nu_e, e^- N'')N'$ and $^{16}O(\bar{\nu}_e, e^+ N'')N'$ case. Here, N' is a nucleus in which ^{16}F or ^{16}N changed after deexcitaion, and N'' is a nucleus emitted by the deexcitation of ^{16}F or ^{16}N. $J^\pi = 0^-$, 1^-, 2^-, 3^-, and 1^+ are ^{16}O states.
[a] The cross section is implemented according to Suzuki et al. (2018) and T. Suzuki (2022, private communication).

which channel the nucleus branches into during deexcitation. In this simulation, we consider 43 excited states, as listed in Table 2, with multiple channels considered for a single excited state. The total of 31 channels considered in SKSNSim is detailed in Table 3. The cross section is implemented according to Suzuki et al. (2018) and T. Suzuki (2022, private communication), and all cross-section values are listed in SKSNSim.

In the case of a neutral-current reaction with oxygen (^{16}O NC), SK is expected to detect Compton electrons from gamma rays emitted during deexcitation, such as from nitrogen or oxygen. In SKSNSim, we only consider states that emit a single gamma ray during the deexcitation of ^{15}N or ^{15}O, as Langanke et al. (1996) specifically consider states of ^{15}N or ^{15}O generated when a single proton or neutron is emitted from ^{16}O. The cross section is implemented according to Langanke et al. (1996) and Kolbe et al. (2002).

2.5. Output Format

This simulation results contain details regarding the interaction channel and particle kinematics for every event. Each neutrino event includes information about the particle type, time, and position of the neutrino interaction, as well as the particle type, direction, and energy of generated particles. This information is available in two data formats: the SK custom format employed in the SK offline analysis package and NUANCE text format,[6] which is widely supported by neutrino detector simulators. For SK, the output information from SKSNSim is transferred to the detector simulation, including simulation of the trigger system, for further assessment of the detector response through the analysis pipeline. Following the simulation, the expected number of events for each interaction is recorded. Specific examples will be provided in the following section.

3. Demonstration

In this section, we describe the demonstration of SKSNSim in its SN burst and DSNB mode. It generates observable particles in water Cherenkov detectors and can pass information about these particles to detector simulators in two modes: the SN burst and the DSNB mode. Section 3.1 provides examples of events generated by neutrino interactions in the SN burst mode and positron events generated by IBD in the DSNB mode. Section 3.2 explains how the generated events can be used for SK analysis.

3.1. Generated Neutrino Events

This section shows the simulation result of an SN burst and a DSNB using SKSNSim. The process begins by calculating the number of events for each interaction, followed by defining the kinematics for each event. Users have the flexibility to change the direction of the neutrino in each event and distance from an SN to a detector. In both modes, the neutrino energy is determined by a random number that follows the energy distribution defined by the model, and the interaction vertex is generated uniformly inside the detector. Furthermore, using the previously determined energy and direction of the neutrino, the kinematics of outgoing particles, such as positrons in the IBD interaction, are determined based on their respective differential cross section.

Figure 2 shows the time, energy, and angular distributions of neutrino events interacting with water in the case of an SN burst. In the SN burst mode, the type of neutrino interaction, its time and vertex, as well as the type of generated particle, its direction, and energy, are stored as event information for a single SN explosion. θ_{SN} represents the angle between neutrinos and a generated particle for each interaction. This case assumes the Nakazato model (Nakazato et al. 2013).

Figure 3 shows an example of positron energy distribution from 100,000 IBD events generated by DSNB under the assumptions made in Horiuchi et al. (2009). The direction of neutrinos is determined isotropically.

3.2. Usage in Super-Kamiokande

This section briefly explains the usage in the SK analysis. The simulator was originally designed for analysis in SK,

[6] The documentation is available on http://neutrino.phy.duke.edu/nuance-format/.

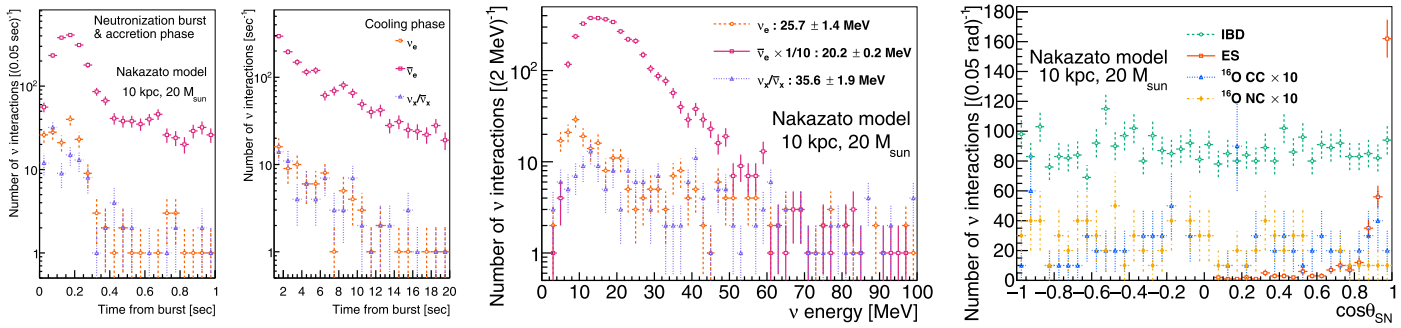

(a) (b) (c)

Figure 2. Distributions of neutrino events generated by a typical SN burst. These distributions show true kinematics without detector response. (a) Timing distributions of generated neutrino events. The left focuses on the neutronization burst and accretion phases. The right figure refers to the cooling phase. (b) Time-integrated energy distribution of generated neutrino events integrated over all phases. The numbers in the legend are the mean energy for each neutrino type. (c) $\theta_{\rm SN}$ distribution between neutrinos and positrons in the IBD case, between neutrinos and electrons in the ES case, between neutrinos and electrons or positrons in the ^{16}O CC case, and between neutrinos and gamma rays in the ^{16}O NC case. The underlying model is that of Nakazato et al. (2013), for which the parameters of the progenitor are mass of $M = 20\,M_{\odot}$, shock revival time of 200 ms, metallicity of $Z = 0.02$, and distance of $d = 10$ kpc. We assume no neutrino oscillation in these plots.

Table 3
List of Channels Included in SKSNSim[a]

Reaction: $^{16}\mathrm{O}(\nu_e, e^- N'')N'$				
$^{16}\mathrm{O}(\nu_e, e^-\gamma)^{16}\mathrm{F}$	$^{16}\mathrm{O}(\nu_e, e^- n)^{15}\mathrm{F}$	...	...	...
$^{16}\mathrm{O}(\nu_e, e^- p)^{15}\mathrm{O}$	$^{16}\mathrm{O}(\nu_e, e^- pn)^{14}\mathrm{O}$	...	...	...
$^{16}\mathrm{O}(\nu_e, e^- 2p)^{14}\mathrm{N}$	$^{16}\mathrm{O}(\nu_e, e^-{}^3\mathrm{He})^{13}\mathrm{N}$	$^{16}\mathrm{O}(\nu_e, e^-\alpha)^{12}\mathrm{N}$	...	...
$^{16}\mathrm{O}(\nu_e, e^- N'')^{13}\mathrm{C}$	$^{16}\mathrm{O}(\nu_e, e^- N'')^{12}\mathrm{C}$	$^{16}\mathrm{O}(\nu_e, e^- p\alpha)^{11}\mathrm{C}$	$^{16}\mathrm{O}(\nu_e, e^- N'')^{10}\mathrm{C}$	...
$^{16}\mathrm{O}(\nu_e, e^- N'')^{12}\mathrm{B}$	$^{16}\mathrm{O}(\nu_e, e^- N'')^{11}\mathrm{B}$	$^{16}\mathrm{O}(\nu_e, e^- N'')^{10}\mathrm{B}$	$^{16}\mathrm{O}(\nu_e, e^- N'')^{9}\mathrm{B}$	...
$^{16}\mathrm{O}(\nu_e, e^- N'')^{11}\mathrm{Be}$	$^{16}\mathrm{O}(\nu_e, e^- N'')^{10}\mathrm{Be}$	$^{16}\mathrm{O}(\nu_e, e^- N'')^{9}\mathrm{Be}$	$^{16}\mathrm{O}(\nu_e, e^- N'')^{8}\mathrm{Be}$	$^{16}\mathrm{O}(\nu_e, e^- N'')^{7}\mathrm{Be}$
$^{16}\mathrm{O}(\nu_e, e^- N'')^{10}\mathrm{Li}$	$^{16}\mathrm{O}(\nu_e, e^- N'')^{9}\mathrm{Li}$	$^{16}\mathrm{O}(\nu_e, e^- N'')^{8}\mathrm{Li}$	$^{16}\mathrm{O}(\nu_e, e^- N'')^{7}\mathrm{Li}$	$^{16}\mathrm{O}(\nu_e, e^- N'')^{6}\mathrm{Li}$
$^{16}\mathrm{O}(\nu_e, e^- N'')^{6}\mathrm{He}$	$^{16}\mathrm{O}(\nu_e, e^- N'')^{5}\mathrm{He}$	$^{16}\mathrm{O}(\nu_e, e^- N'')^{4}\mathrm{He}$	$^{16}\mathrm{O}(\nu_e, e^- N'')^{3}\mathrm{He}$	...
$^{16}\mathrm{O}(\nu_e, e^- N'')^{3}\mathrm{H}$	$^{16}\mathrm{O}(\nu_e, e^- N'')^{2}\mathrm{H}$	...	...	...
Reaction: $^{16}\mathrm{O}(\bar{\nu}_e, e^+ N'')N'$				
$^{16}\mathrm{O}(\bar{\nu}_e, e^+\gamma)^{16}\mathrm{N}$	$^{16}\mathrm{O}(\bar{\nu}_e, e^+ n)^{15}\mathrm{N}$	$^{16}\mathrm{O}(\bar{\nu}_e, e^+ 2n)^{14}\mathrm{N}$	$^{16}\mathrm{O}(\bar{\nu}_e, e^+ N'')^{13}\mathrm{N}$	...
$^{16}\mathrm{O}(\bar{\nu}_e, e^+ pn)^{14}\mathrm{C}$	$^{16}\mathrm{O}(\bar{\nu}_e, e^+{}^3\mathrm{H})^{13}\mathrm{C}$	$^{16}\mathrm{O}(\bar{\nu}_e, e^+ N'')^{12}\mathrm{C}$	$^{16}\mathrm{O}(\bar{\nu}_e, e^+ N'')^{11}\mathrm{C}$	$^{16}\mathrm{O}(\bar{\nu}_e, e^+ N'')^{10}\mathrm{C}$
$^{16}\mathrm{O}(\bar{\nu}_e, e^+ N'')^{14}\mathrm{B}$	$^{16}\mathrm{O}(\bar{\nu}_e, e^+ N'')^{13}\mathrm{B}$	$^{16}\mathrm{O}(\bar{\nu}_e, e^+\alpha)^{12}\mathrm{B}$	$^{16}\mathrm{O}(\bar{\nu}_e, e^+ N'')^{11}\mathrm{B}$	$^{16}\mathrm{O}(\bar{\nu}_e, e^+ N'')^{10}\mathrm{B}$
$^{16}\mathrm{O}(\bar{\nu}_e, e^+ N'')^{9}\mathrm{B}$	$^{16}\mathrm{O}(\bar{\nu}_e, e^+ N'')^{8}\mathrm{B}$	...	...	...
$^{16}\mathrm{O}(\bar{\nu}_e, e^+ N'')^{12}\mathrm{Be}$	$^{16}\mathrm{O}(\bar{\nu}_e, e^+ N'')^{11}\mathrm{Be}$	$^{16}\mathrm{O}(\bar{\nu}_e, e^+ N'')^{10}\mathrm{Be}$	$^{16}\mathrm{O}(\bar{\nu}_e, e^+ N'')^{9}\mathrm{Be}$	$^{16}\mathrm{O}(\bar{\nu}_e, e^+ N'')^{8}\mathrm{Be}$
$^{16}\mathrm{O}(\bar{\nu}_e, e^+ N'')^{7}\mathrm{Be}$	...	...	...	...
$^{16}\mathrm{O}(\bar{\nu}_e, e^+ N'')^{9}\mathrm{Li}$	$^{16}\mathrm{O}(\bar{\nu}_e, e^+ N'')^{8}\mathrm{Li}$	$^{16}\mathrm{O}(\bar{\nu}_e, e^+ N'')^{7}\mathrm{Li}$	$^{16}\mathrm{O}(\bar{\nu}_e, e^+ N'')^{6}\mathrm{Li}$	...
$^{16}\mathrm{O}(\bar{\nu}_e, e^+ N'')^{6}\mathrm{He}$	$^{16}\mathrm{O}(\bar{\nu}_e, e^+ N'')^{4}\mathrm{He}$	$^{16}\mathrm{O}(\bar{\nu}_e, e^+ N'')^{3}\mathrm{He}$	...	...
$^{16}\mathrm{O}(\bar{\nu}_e, e^+ N'')^{3}\mathrm{H}$	$^{16}\mathrm{O}(\bar{\nu}_e, e^+ N'')^{2}\mathrm{H}$	...	...	...

Note. This table shows channels for $^{16}\mathrm{O}(\nu_e, e^- N'')N'$ and $^{16}\mathrm{O}(\bar{\nu}_e, e^+ N'')N'$ cases. Here, N' is a nucleus in which ^{16}F or ^{16}N changed after deexcitation, and N'' is a nucleus emitted by deexcitation of ^{16}F or ^{16}N.
[a] The cross section is implemented according to Suzuki et al. (2018) and T. Suzuki (2022, private communication).

especially for sensitivity calculations to the SN burst (Kashiwagi et al. 2024) and the optimization of the DSNB analysis (Harada et al. 2023). The pipeline for the analysis consists of a neutrino interaction part (SKSNSim), the full detector simulation of generated particles, and the detailed analysis for specific studies. The SK software package holds an internal data format that is consistent throughout the tool-processing pipeline using the ROOT package (Brun & Rademakers 1997). The SK detector simulator simulates the detector response for particles generated in neutrino interactions, which are the output of SKSNSim.

In the case of an SN burst, the simulation flow is straightforward. SKSNSim generates the neutrino event information, and the detector simulator processes the output for each neutrino event. After that, the time series of neutrino events is considered. SK observes Cherenkov photons emitted by charged particles generated in a neutrino interaction. These photons may overlap with each other in neutrino events, especially under high event rates during the early phase. For this reason, the detected photons are ordered by arrival time independently of the neutrino event, and after being combined with the continuous detector noise, a trigger simulation is applied. After being reconstructed as SK events by the trigger simulation, the timing profile and energy of neutrino emission from the SN burst and the direction of the original SN source are estimated (Kashiwagi et al. 2024).

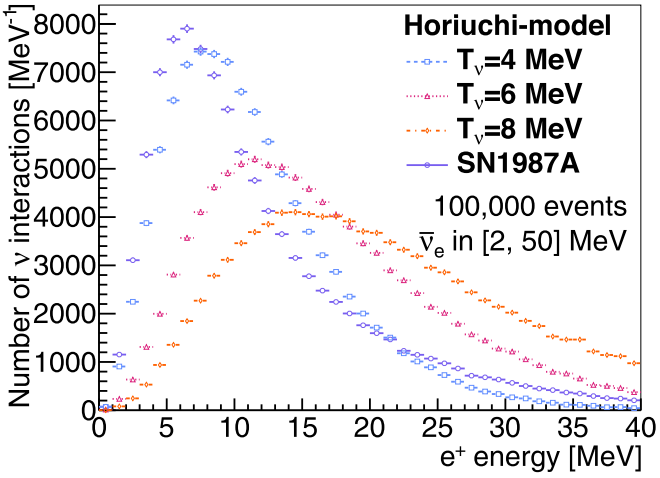

Figure 3. Energy spectra of positrons generated by DSNB with water via the IBD channel. Here, the calculation of Horiuchi et al. (2009) is used for the DSNB model and that of Strumia & Vissani (2003) is used for the IBD cross section. The Horiuchi model provides several cases with different effective temperatures (T_ν) in the SN core: 4, 6, and 8 MeV in this plot.

In contrast, the DSNB process uses a different procedure (Harada et al. 2023). In the step of SKSNSim, we first generate the necessary number of positron events, assuming that the positron energy distribution is flat, and then determine the original $\bar{\nu}_e$ kinematics by throwing in a random number according to the IBD differential cross section for each positron event. Each positron event is weighted according to the original neutrino energy distribution when making the positron energy distribution in the analysis pipeline. This method is called the "reweighting" method. It can be applied with any $\bar{\nu}_e$ spectrum, for example, $\bar{\nu}_e$ from reactors, because only the IBD interaction of $\bar{\nu}_e$ is considered.

4. Summary

SKSNSim is a collection of software to simulate neutrino interaction events of SN bursts and DSNB. We have developed SKSNSim originally for SK and modified it for general purposes and public use. In this paper, we described the basic structures. It outputs the interaction position and the outgoing particles' type, direction, and energy according to the differential cross section of neutrino interactions in the water. Based on this output information, the detector simulator traces the Cherenkov photons emitted from the interacted particles. We demonstrated SKSNSim in both SN bursts and DSNBs and explained how it is used in these analyses. It applies to any water-based detector, for example, the Hyper-Kamiokande detector, which is now under construction (Wilson 2022).

Acknowledgments

We would like to thank Y. Kashiwagi for providing the text data of the SN burst models and T. Suzuki for many useful suggestions about oxygen-excited states after neutrino interactions. We are also grateful for helpful discussions with K. Scholberg, M. Nakahata, H. Sekiya, M. Ikeda, and G. Pronost. This work is supported by JSPS KAKENHI grant No. JP23KJ1609, JP23KJ0890, JP20J20189, and JP20H00162. This work was supported by JST, the establishment of university fellowships toward the creation of science technology innovation, grant No. JPMJFS2112.

ORCID iDs

Fumi Nakanishi https://orcid.org/0000-0003-4408-6929
Shota Izumiyama https://orcid.org/0000-0002-0808-8022
Masayuki Harada https://orcid.org/0000-0003-3273-946X
Yusuke Koshio https://orcid.org/0000-0003-0437-8505

References

Aartsen, M. G., Ackermann, M., Adams, J., et al. 2017, JInst, 12, P03012
Abe, K., Bronner, C., Hayato, Y., et al. 2022, NIMPA, 1027, 166248
Adrián-Martínez, S., Ageron, M., Aharonian, F., et al. 2016, JPhG, 43, 084001
Al Kharusi, S., BenZvi, S. Y., Bobowski, J. S., et al. 2021, NJPh, 23, 031201
Alexeyev, E. N., Alexeyeva, L. N., Krivosheina, I. V., & Volchenko, V. I. 1988, PhLB, 205, 209
Bahcall, J. N., Kamionkowski, M., & Sirlin, A. 1995, PhRvD, 51, 6146
Baxter, A. L., Benzvi, S., Jaimes, J. C., et al. 2022, ApJ, 925, 107
Bionta, R. M., Blewitt, G., Bratton, C. B., et al. 1987, PhRvL, 58, 1494
Brun, R., & Rademakers, F. 1997, NIMPA, 389, 81
Burrows, A., Radice, D., Vartanyan, D., et al. 2020, MNRAS, 491, 2715
Burrows, A., & Vartanyan, D. 2021, Natur, 589, 29
Dighe, A. S., & Smirnov, A. Y. 2000, PhRvD, 62, 033007
Duan, H., Fuller, G. M., & Qian, Y.-Z. 2010, ARNPS, 60, 569
Fischer, T., Whitehouse, S. C., Mezzacappa, A., Thielemann, F. K., & Liebendörfer, M. 2010, A&A, 517, A80
Fukuda, S., Fukuda, Y., Hayakawa, T., et al. 2003, NIMPA, 501, 418
Hanke, F., Müller, B., Wongwathanarat, A., Marek, A., & Janka, H.-T. 2013, ApJ, 770, 66
Harada, M., Abe, K., Bronner, C., et al. 2023, ApJL, 951, L27
Hartmann, D. H., & Woosley, S. E. 1997, APh, 7, 137
Hirata, K., Kajita, T., Koshiba, M., et al. 1987, PhRvL, 58, 1490
Horiuchi, S., Beacom, J. F., & Dwek, E. 2009, PhRvD, 79, 083013
Kashiwagi, Y., Abe, K., Bronner, C., et al. 2024, arXiv:2403.06760
Kolbe, E., Langanke, K., & Vogel, P. 2002, PhRvD, 66, 013007
Langanke, K., Vogel, P., & Kolbe, E. 1996, PhRvL, 76, 2629
Malaney, R. A. 1997, APh, 7, 125
Migenda, J., Cartwright, S., Kneale, L., et al. 2021, JOSS, 6, 2877
Mikheyev, S. P., & Smirnov, A. Y. 1985, YaFiz, 42, 1441
Mori, M., Suwa, Y., Nakazato, K., et al. 2021, PTEP, 2021, 023E01
Nakazato, K., Sumiyoshi, K., Suzuki, H., et al. 2013, ApJS, 205, 2
Nakazato, K., Suzuki, T., & Sakuda, M. 2018, PTEP, 2018, 123E02
Nomoto, K. 1987, ApJ, 322, 206
Ricciardi, G., Vignaroli, N., & Vissani, F. 2022, JHEP, 2022, 212
Scholberg, K., Albert, J. B., & Vasel, J., 2021 SNOwGLoBES: SuperNova Observatories with GLoBES, Astrophysics Source Code Library, ascl:2109.019
Strumia, A., & Vissani, F. 2003, PhLB, 564, 42
Suzuki, A. 2014, EPJC, 74, 3094
Suzuki, T., Chiba, S., Yoshida, T., Takahashi, K., & Umeda, H. 2018, PhRvC, 98, 034613
Takiwaki, T., Kotake, K., & Suwa, Y. 2012, ApJ, 749, 98
Tamborra, I., Raffelt, G., Hanke, F., Janka, H.-T., & Müller, B. 2014, PhRvD, 90, 045032
Totani, T., Sato, K., Dalhed, H. E., & Wilson, J. R. 1998, ApJ, 496, 216
Vogel, P., & Beacom, J. F. 1999, PhRvD, 60, 053003
Wilson, J. 2022, Accelerator Neutrino II_Hyper-K v1, Zenodo, doi:10.5281/ZENODO.6693820
Wolfenstein, L. 1978, PhRvD, 17, 2369